14. Chu, Y., Wang, Z., Gu, D. and Yin, G., Performance of Pt/C catalysts prepared by microwave-assisted polyol process form ethanol electrooxidation. *J. Power Sources*, 2010, **195**, 1799–1804.
15. Vinayan, B. P., Nagar, R., Rajalakshmi, N. and Ramaprabhu, S., Novel platinum–cobalt alloy nanoparticles dispersed on nitrogen-doped grapheme as a cathode electrocatalyst for PEFMC applications. *Adv. Funct. Mater*., 2012, **22**, 3519–3526.
16. Hu, S., Xiong L., Ren, X., Wang, C. and Luo, Y., Pt–Ir binary hydrophobic catalyst: effects of Ir content and particle size on catalytic performance for liquid phase catalytic exchange. *Int. J. Hydrogen Energy*, 2009, **34**, 8723–8732.
17. Ye, L., Luo, D., Yang, W., Guo, W., Xu, Q. and Jiang, C., Improved catalysts for hydrogen/deuterium exchange reactions. *Int. J. Hydrogen Energy*, 2013, **38**, 13596–13603.

ACKNOWLEDGEMENTS. We thank Shri Tulsiram, Shri B. P. Dubey, P Kumawat (Heavy Water Plant, Baroda) for carrying out the catalytic activity measurements and Shri Rajnish Prakash (Heavy Water Board) for encouragement and support. We also thank Shri Gopal Mohod (RRCAT, Indore) for assistance.

Received 1 May 2015; revised accepted 30 July 2015

doi: 10.18520/v109/i10/1860-1864

Gravitational attraction of a vertical pyramid model of flat top and bottom with depth-wise linear density variation

Anand P. Gokula and Rambhatla G. Sastry*

Department of Earth Sciences, Indian Institute of Technology, Roorkee 247 667, India

In 3D gravity modelling, a right rectangular parallelepiped with either constant density or variable density functions in spatial and spectral domains enjoys wide popularity. However, better unit models are needed to meet the large variety of geological scenarios. Here, we present an analytical expression for the gravity effect of a vertical pyramid model with depth-wise linear density variation. Initially, we validate our analytic expression against the gravity effect of a right rectangular parallelepiped and provide two synthetic examples and a case study for illustrating the effectiveness of our pyramid model in gravity modelling. The included case study of Los Angeles basin, California, USA, demonstrates the comparative advantages of our pyramid model over the conventional right rectangular vertical prism model. Thus, our pyramid model could be quiet effective as a building block for evaluating the gravity effect of an arbitrarily-shaped 3D or 2.5D source(s).

Keywords: Gravitational attraction, linear density variation, right rectangular, parallelepiped model, vertical pyramid model.

THE evaluation of theoretical gravity response of 3D targets is an involved process requiring considerable theoretical and computational efforts. Several authors have addressed this problem in both spatial[1–4] and spectral domains[5,6]. The polygonal lamina model[4], the right rectangular prism model with constant density contrast[1,3], and the right rectangular prism model with parabolic density variation depth-wise[2] have enjoyed wide popularity. However, for real geological applications, one needs better 3D unit models.

Starostenko[7] has proposed an inhomogeneous vertical pyramid model with flat top and bottom and sloping sides possessing a linear density variation depth-wise. However, he was unable to derive a complete analytical expression for its gravity effect.

Here, we derive the complete gravity expression for the same pyramid model and illustrate its effectiveness through two synthetic examples after customary validation check of our forward problem solution.

Consider an isolated regular pyramid model *ABCDEFGH* with flat top *ABCD* and bottom surface, EFGH (Figure 1 *a*). The gravity effect of such a model at any arbitrary point (x, y, z) in free space[7] is given by

$$g_{\text{pyramid}}(x, y, z) = \gamma \int_{\zeta=h_1}^{h_2} \int_{\eta=\eta_l}^{\eta_u} \int_{\xi=\xi_l}^{\xi_u} \frac{\sigma(\zeta)(\zeta - z)\mathrm{d}\xi\mathrm{d}\eta\mathrm{d}\zeta}{((\xi - x)^2 + (\eta - y)^2 + (\zeta - z)^2)^{3/2}}, \quad (1)$$

where

$$\left.\begin{aligned} \sigma(\zeta) &= \sigma + k(\zeta - h_1), \\ \xi_l &= (h_1 - \zeta)(\xi_1 - \xi_3)/(h_2 - h_1) + \xi_1, \\ \xi_u &= (h_1 - \zeta)(\xi_2 - \xi_4)/(h_2 - h_1) + \xi_2, \\ \eta_l &= (h_1 - \zeta)(\eta_1 - \eta_3)/(h_2 - h_1) + \eta_1, \\ \eta_u &= (h_1 - \zeta)(\eta_2 - \eta_4)/(h_2 - h_1) + \eta_2. \end{aligned}\right\}, \quad (2)$$

where σ is constant density (g/cm^3), k the linear coefficient (g/cm^3/km), γ the universal gravitational constant, h_1 and h_2 are the depth of the top and bottom surfaces of pyramid respectively, and ζ refers to depth below h_1. $A(\xi_1, \eta_1, h_1)$, $B(\xi_1, \eta_2, h_1)$, $C(\xi_2, \eta_2, h_1)$, $D(\xi_2, \eta_1, h_1)$, $E(\xi_3, \eta_3, h_2)$, $F(\xi_3, \eta_4, h_2)$, $G(\xi_4, \eta_4, h_2)$ and $H(\xi_3, \eta_3, h_2)$ are the corners of the pyramid (Figure 1 *a*). By changing

*For correspondence. (e-mail: rgss1fes@iitr.ac.in)

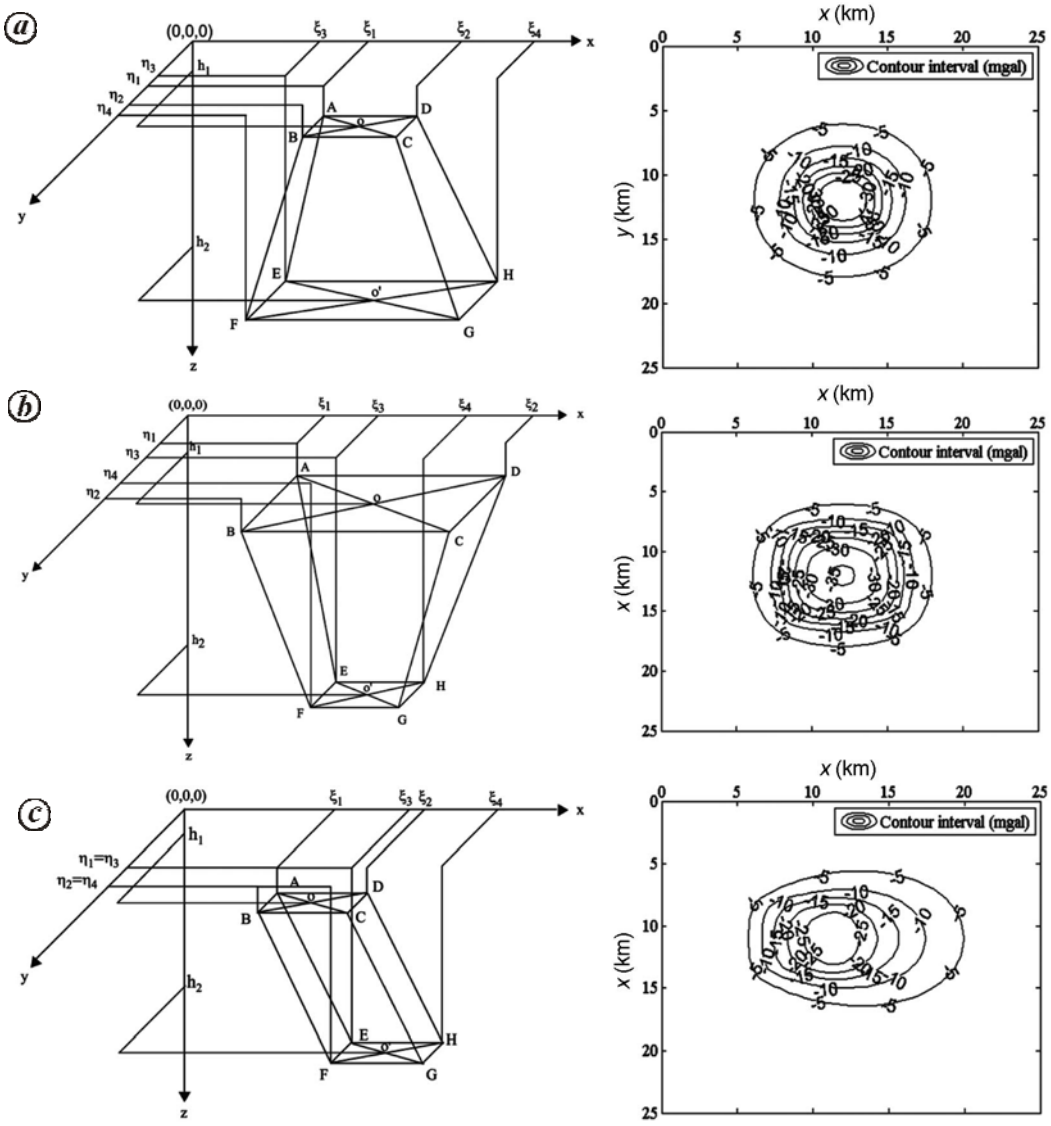

Figure 1. 3D pyramid models and their geometries with depth-wise linear density variation and their gravity effects. The pyramid model parameters are as follows: (***a***) $\xi_1 = 10$, $\xi_2 = 14$, $\xi_3 = 8$, $\xi_4 = 16$, $\eta_1 = 10$, $\eta_2 = 14$, $\eta_3 = 8$, $\eta_4 = 16$; (***b***) $\xi_1 = 8$, $\xi_2 = 16$, $\xi_3 = 10$, $\xi_4 = 14$, $\eta_1 = 8$, $\eta_2 = 16$, $\eta_3 = 10$, $\eta_4 = 14$, and (***c***) $\xi_1 = 6$, $\xi_2 = 12$, $\xi_3 = 15$, $\xi_4 = 21$, $\eta_1 = 8$, $\eta_2 = 14$, $\eta_3 = 8$, $\eta_4 = 14$. Parameters $\sigma = -0.5206$ g/cm^3, $k = 0.0403$ g/cm^3/km, $h_1 = 0.5$, $h_2 = 5$ and $z = 0$ remain the same for all three models. All length parameters and station distances are expressed in kilometres.

the variables on the right hand side (RHS) in eqs (1) and (2) i.e.

$$\xi - x = \xi'; \ \eta - y = \eta'; \ \zeta - z = \zeta',$$

we get

$$g_{\text{pyramid}}(x, y, z) = \gamma \int_{\zeta'=h_1-z}^{h_2-z} \int_{\eta'=\eta'_l-y}^{\eta'_u-y} \int_{\xi'=\xi'_l-x}^{\xi'_u-x} \frac{\sigma(\zeta')\zeta' \mathrm{d}\xi' \mathrm{d}\eta' \mathrm{d}\zeta'}{R^3}, \tag{3}$$

where

$$\left.\begin{aligned} \sigma(\zeta') &= \sigma + k(\zeta' + z - h_1), \\ \xi'_l &= (h_1 - \zeta' - z)(\xi_1 - \xi_3)/(h_2 - h_1) + \xi_1, \\ \xi'_u &= (h_1 - \zeta' - z)(\xi_2 - \xi_4)/(h_2 - h_1) + \xi_2, \\ \eta'_l &= (h_1 - \zeta' - z)(\eta_1 - \eta_3)/(h_2 - h_1) + \eta_1, \\ \eta'_u &= (h_1 - \zeta' - z)(\eta_2 - \eta_4)/(h_2 - h_1) + \eta_2, \\ R &= \sqrt{(\xi')^2 + (\eta')^2 + (\zeta')^2}. \end{aligned}\right\} \tag{4}$$

Equation (3) shows the mathematical expression for pyramid model in integral form. Supplementary Information contains the final analytical expression (forward problem solution) with relevant mathematical details.

Table 1. Linear density models and error estimates of gravity forward modelling

Linear density model	σ (g/cm^3)	k (g/cm^3/km)	RMS error between observed and computed (in the present study) gravity anomaly (mgal)	NRMS error between observed and computed (in the present study) gravity anomaly	RMS error between observed and computed (by Chakravarthi *et al.*[2]) gravity anomaly (mgal)	NRMS error between observed and computed (by Chakravarthi *et al.*[2]) gravity anomaly
Model 1	–0.5206	0.0510	8.6287	0.1095	12.0919	0.1778
Model 2	–0.5206	0.0403	9.8926	0.1147		
Model 3	–0.4100	0.0400	10.9660	0.1763		
Model 4	–0.4653	0.04015	8.3788	0.1129		

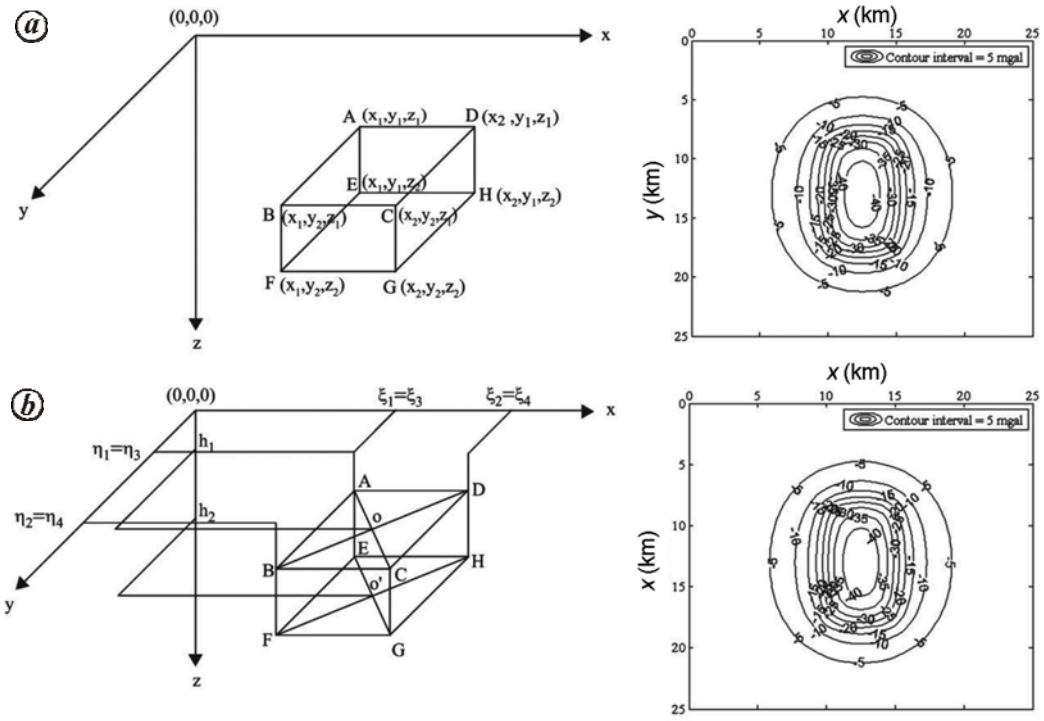

Figure 2. Validation of our forward problem solution (eq. (A6), see Supplementary Information online) through comparison of gravity response with that of right rectangular parallelepiped[1]. ***a***, Geometry and gravity anomaly plot of right rectangular parallelepiped[1]. The parameters are as follows: $x_1 = 10$, $x_2 = 15$, $y_1 = 8$, $y_2 = 18$, $z_1 = 0.5$, $z_2 = 5$ and $\rho = -0.5206$ g/cm^3. ***b***, Geometry and gravity anomaly plot of our pyramid model. The pyramid model parameters are as follows: $\xi_1 = 10$, $\xi_2 = 15$, $\xi_3 = 10$, $\xi_4 = 15$, $\eta_1 = 8$, $\eta_2 = 18$, $\eta_3 = 8$, $\eta_4 = 18$, $h_1 = 0.5$, $h_2 = 5$, $\sigma = -0.5206$ g/cm^3 and $k = 0$. All length parameters and station distances are expressed in kilometres.

The integral evaluations on the RHS of eq. (3) were undertaken using Wolfram Mathematica 9.0.1. Drafting of illustrations was implemented through MATLAB 2013b.

Figure 1 shows the geometry and gravity anomaly plot for a single pyramid model and it serves as an initial example.

To validate our gravity forward problem solution (see eq. A6, Supplementary Information online) for a pyramid model, we have considered a single right rectangular parallelepiped with constant density[1], whose gravity effect at the origin (Figure 2 *a*) is given by

$$g_z(0,0,0) = \gamma\rho \left[x \ln(y + \sqrt{x^2 + y^2 + z^2}) + y \ln(x + \sqrt{x^2 + y^2 + z^2}) - z \tan^{-1} \frac{xy}{z\sqrt{x^2 + y^2 + z^2}} \right] \Bigg|_{x_1}^{x_2} \Bigg|_{y_1}^{y_2} \Bigg|_{z_1}^{z_2}, \quad (5)$$

where γ is the universal gravitational constant and ρ is the constant density of the prism (g/cm^3).

Our analytical expression for the pyramid (eq. A6, See Supplementary Information online) gets reduced to that of eq. (5) for the linear coefficient $k = 0$ and by adjusting coordinates of pyramid vertices (Figure 1).

Accordingly, Figure 2 *a* corresponds to the gravity effect of a right rectangular parallelepiped[1], while Figure 2 *b* to that of the present model. Our model response matches

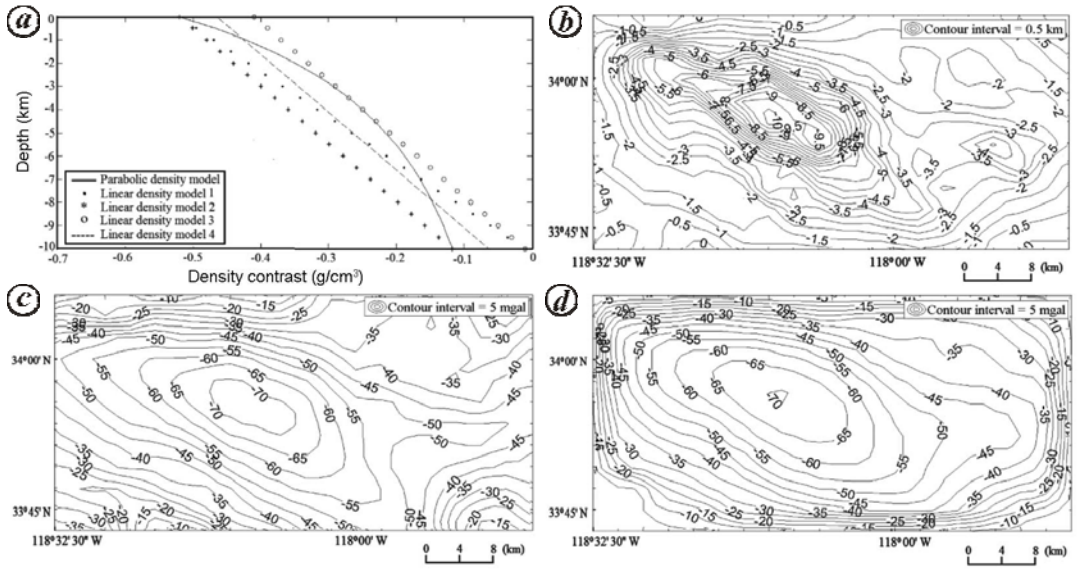

Figure 3. ***a***, Four linear density models for a parabolic density function opted by Chakravarthi *et al.*[2]. The values of constant density (σ) at the surface and linear coefficient (k) are given in Table 1. ***b***, Basement topography of the Los Angeles basin, California, USA[8]. ***c***, Residual gravity anomaly map of Los Angeles basin[8]. ***d***, Computed gravity anomaly map of Los Angeles basin, using 3D vertical prism with parabolic density function[2].

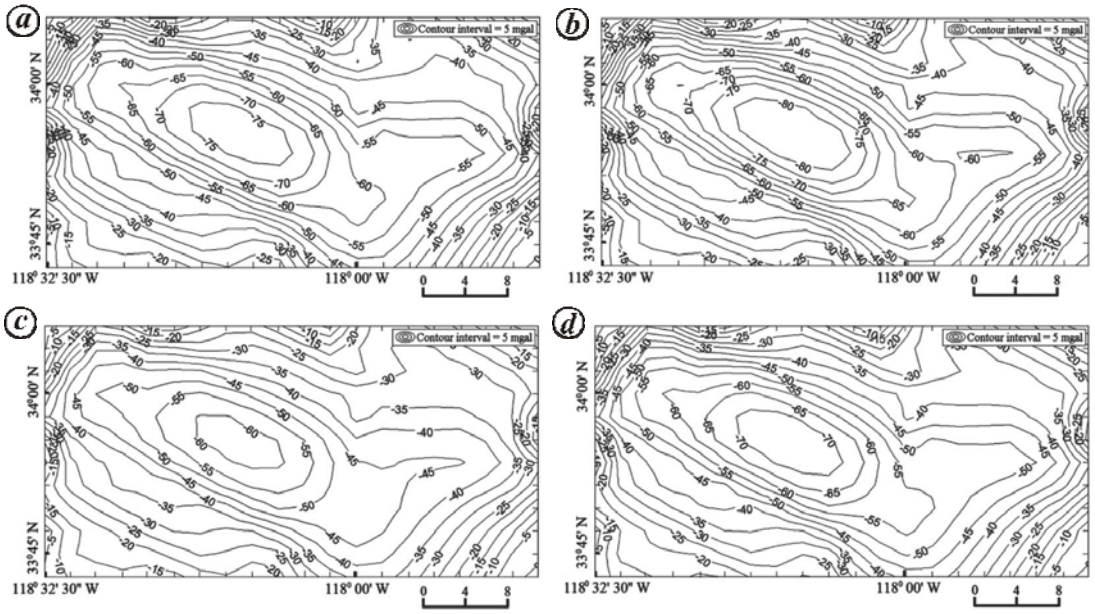

Figure 4. Computed gravity anomaly map of Los Angeles basin using vertical pyramid model with linear density function (***a***) for model 1 (σ = –0.5206 and k = 0.0510); (***b***) for model 2 (σ = –0.5206 and k = 0.0403); (***c***) for model 3 (σ = –0.410 and k = 0.0400); (***d***) for model 4 (σ = –0.4653 and k = 0.04015).

well with that of the right rectangular parallelepiped (root mean square (RMS) error = 1.210×10^{-4} and normalized root mean square (NRMS) error = 2.816×10^{-6}).

For illustration purpose, we have included two synthetic pyramid models and their computed gravity effects in Figure 1 *b* and *c*, based on eq. A6 (see Supplementary Information online).

The case study concerns gravity modelling of the Los Angeles Basin, California, USA[2,8].

The logic for generating these linear density models from parabolic density model[2] is illustrating in Figure 3 *a* and relevant details are included in Table 1. By considering the basement surface contour map (Figure 3 b) of the Los Angeles basin as input[8], we have carried out forward modelling for four different linear density models (Figures 3 *a* and 4). We have digitized the basement topographic map[8] (Figure 3 *b*) for forward modelling, residual gravity anomaly map[8] (Figure 3 *c*) and theoretical gravity

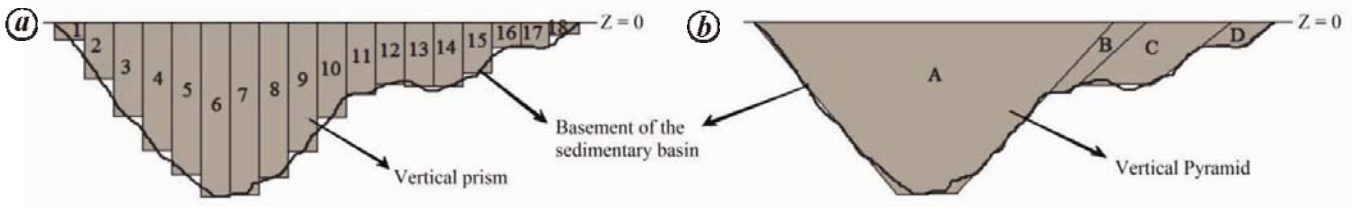

Figure 5. Schematic demonstration of model discretization for approximating arbitrary geometry of gravity anomaly source using (***a***) conventional vertical prism model and (***b***) Vertical pyramid model.

anomaly map[2] (Figure 3 *d*) of Los Angeles basin on 2×2 km^2 grid for comparison purpose.

We have carried out forward modelling for all four linear density model (Table 1) and their results are included in Figure 4. Table 1 also contains error estimates of our forward modelling efforts relative to that of Chakravarthi *et al.*[2].

Our theoretical gravity expression for a pyramid model with sloping sides is validated against that of a right rectangular parallelepiped model[1]. It may be noted that at validation stage, to avoid numerical difficulties, we have perturbed the coordinates of bottom surface vertices of the model by a small amount (10^{-4} km in our case).

In our case study, as the parabolic density model of Chakravarthi *et al.*[2] needs to be accommodated by a proper linear density model, necessary care has been taken by devising four independent linear density models (Figure 3 *a* and Table 1). Figure 3 *b–d* respectively, outlines the case study of Chakravarthi *et al.*[2]. The criterion for proper choice of linear density model is judged by RMS and NRMS error estimates. By considering the procedure of Chakravarthi *et al.*[2], one needs a minimum of 209 3D vertical prisms for modelling the Los Angeles basin. However, using our pyramid model, only 10 individual pyramids are needed to achieve better accuracy. Table 1 and Figure 4 illustrate that higher accuracy is achieved in the case of linear density model 4 (Figure 4 *d*).

Our pyramid model (Figure 1 *a*) offers better approximation and ease in implementing gravity forward modelling for both 3D and 2.5D cases. For present-day computer infrastructure, complicated analytic expressions such as eqs (5) and (A6; Supplementary Information) do not pose any computational problem (CPU time). Figure 5 schematically illustrates that our model discretization scores over that of Chakravarthi *et al.*[2].

A theoretical gravity anomaly expression is devised for a 3D vertical pyramid model with linear density variation with depth. Our theoretical gravity expression for a pyramid model with sloping sides is validated against that of the right rectangular parallelepiped model[1]. We have also implemented two synthetic experiments and one case study, which demonstrate the utility of our forward problem solution.

The proposed pyramid model and its gravity response are quiet effective as a building block for computing the gravity effect of an arbitrarily-shaped 3D or 2.5D source(s) in comparison to that of conventional rectangular parallelepiped model.

The relevant derivations of tensorial gravity components and magnetic anomaly expressions for the pyramid model are underway.

1. Banerjee, B. and Das Gupta, S. P., Short note: gravitational attraction of a rectangular parallelepiped. *Geophysics*, 1997, **42**, 1053–1055.
2. Chakravarthi, V., Raghuram, H. M. and Singh, S. B., Short note: 3-D forward modelling of basement interfaces above which the density contrast varies continuously with depth. *Comput. Geosci.*, 2002, **28**, 53–57.
3. Nagy, D., The gravitational attraction of a right rectangular prism. *Geophysics*, 1966, **30**, 362–371.
4. Talwani, M. and Ewing, M., Rapid computation of gravitational attraction of three-dimensional bodies of arbitrary shape. *Geophysics*, 1960, **25**, 203–225.
5. Bhattacharyya, B. K. and Leu, L. K., Spectral analysis of gravity and magnetic anomalies due to rectangular prismatic bodies. *Geophysics*, 1997, **42**, 41–50.
6. Bhattacharyya, B. K. and Navolio, M. E., A fast Fourier transform method for rapid computation of gravity and magnetic anomalies due to arbitrary bodies. *Geophys. Prospect.*, 1976, **24**, 633–649.
7. Starostenko, V. I., Inhomogeneous four-cornered vertical pyramid with flat top and bottom surface. In *Stable Computational Method in Gravimetric Problems* (*in Russian*), Navukova Dumka, Kiev, Russia, 1978, pp. 90–95.
8. Chai, Y. and Hinze, W. J., Gravity inversion of an interface above which the density contrast varies exponentially with depth. *Geophysics*, 1988, **53**, 837–845.

ACKNOWLEDGEMENTS. The integral evaluations in our formulation of gravity forward problem are undertaken by Wolfram Mathematica 9.0.1. Drafting of illustrations in our paper are implemented through MATLAB 2013b. Mr Anand P. Gokula is thankful to Ministry of Human Resources Development (MHRD), Government of India for financial support.

Received 27 August 2014; revised accepted 30 July 2015

doi: 10.18520/v109/i10/1864-1868